

Selective optical manipulation of the spin state of a single magnetic impurity in a semiconductor quantum dot

Alexander O. Govorov¹ and Alexander V. Kalameitsev²

¹*Department of Physics and Astronomy, Condensed Matter and Surface Science Program,
Ohio University, Athens, Ohio 45701-2979*

²*Institute of Semiconductor Physics, Novosibirsk, 630090 Russia*

(Dated: November 14, 2018)

We describe the optical resonant manipulation of a single magnetic impurity in a self-assembled quantum dot. We show that using the resonant pumping one can address and manipulate selectively individual spin states of a magnetic impurity. The mechanisms of resonant optical polarization of a single impurity in a quantum dot involve anisotropic exchange interactions and are different to those in diluted semiconductors. A Mn impurity can act as qubit. The limiting factors for the qubit manipulation are the electron-hole exchange interaction and finite temperature.

The spins of electrons in semiconductors strongly couple with electric and magnetic fields due to the spin-orbit and exchange interactions. Spintronics and quantum computation utilize these interactions to manipulate the electron spins^{1,2}. One important class of spintronics materials is diluted magnetic semiconductors³ which combine high-quality semiconductor structures with magnetic properties of impurities. Since many semiconductors efficiently emit and absorb light, the spin states of electrons and magnetic impurities can be manipulated optically by using circularly-polarized light pulses⁴. In diluted magnetic semiconductors such as bulk crystals, quantum wells and dots, photo-generated excitons interact with a large collection of spins of Mn impurities and therefore a large number of degrees of freedom becomes involved^{5,6,7,8,9,10,11}. In these systems, it is challenging to address individual spins of Mn atoms. At the same time, the quantum computational schemes are based on qubits, pairs of well-controlled quantum states. These elementary blocks, qubits, should be made interacting or decoupled on demand. In a diluted magnetic semiconductor, even a single Mn atom has 6 spin states ($I_{Mn} = 5/3$). Therefore, 15 different pairs of states (qubits) can be defined for a single Mn impurity. Here we study a system which allows us to manipulate optically a single Mn spin. This system is composed of a quantum dot (QD) and a single Mn impurity. Note that the optical properties of a QD with a single Mn impurity were recently discussed in refs.^{12,13}.

This letter describes a single Mn impurity embedded into a self-assembled QD. Importantly, such a system permits efficient selective optical control and manipulation of individual spin states and defining a single qubit for the Mn impurity. This ability comes from the exciton spectrum of a QD with a Mn atom. An exciton in a QD has a well-defined discrete spectrum and, simultaneously, strongly interacts with the Mn spin via the exchange interaction. Since the exciton and Mn spin functions become strongly mixed, the resonant optical excitation strongly affect the spin state of Mn impurity. In particular, we show that one can *write* spin states of Mn atom. Since spin relaxation of paramagnetic ions in

the absence of carriers (i.e. after the exciton recombination) is an extremely slow process ($\sim 10 \mu s$), a single Mn spin is a very promising candidate for spintronics applications. The mechanisms of Mn-spin polarization in a QD are qualitatively different to those in bulk materials because of the discrete character of quantum states. In bulk, the photo-generated spin-polarized electrons transfer their spin to the Mn atoms or induce an effective magnetic field which polarizes the impurity system⁷. In a QD, the spin orientation of Mn atom comes from the three-body interactions involving an electron, hole, and Mn spin. The ability to manipulate a pair of chosen states (qubit) comes from the resonant excitation of a certain spin state of the exciton-Mn system. In addition, we describe the specific optical signatures of a Mn atom embedded into a QD. In contrast to the undoped self-assembled quantum dots, the optical emission of a laterally-asymmetric quantum dot becomes *circularly polarized* due to the exciton-Mn interaction.

We now consider a model of disk-shaped self-assembled QD taking into account only the heavy holes (HH) states in the valence band. The QD potential strongly confines the electron and HH envelope wave functions, $\phi_e(\mathbf{r}_e)$ and $\phi_h(\mathbf{r}_h)$ and the exchange interactions in the exciton determine the spin state of exciton. According to the conventional model, the Mn-hole and Mn-electron exchange interactions are proportional to $\delta(\mathbf{r}_{e(h)} - \mathbf{R}_{Mn})$, where \mathbf{R}_{Mn} is the Mn position and $\mathbf{r}_{e(h)}$ is the electron (hole) coordinate. Then, the spin Hamiltonian takes the form

$$\hat{H}_{spin} = \hat{H}_{Mn-hole}^{exc} + \hat{H}_{Mn-e}^{exc} + \hat{H}_{e-hole}^{exc}, \quad (1)$$

which includes three types of exchange interaction. The anisotropic exchange interaction between the Mn spin and HH is $\hat{H}_{Mn-hole}^{exc} = \frac{\beta}{3} |\phi_h(\mathbf{R}_{Mn})|^2 \hat{j}_{h,z} \hat{I}_{Mn,z} = A_h \hat{j}_{h,z} \hat{I}_{Mn,z}$; the Mn-electron interaction is isotropic, $\hat{H}_{Mn-e}^{exc} = \alpha |\phi_e(\mathbf{R}_{Mn})|^2 \hat{\mathbf{s}} \hat{\mathbf{I}}_{Mn} = A_e \hat{\mathbf{s}} \hat{\mathbf{I}}_{Mn}$. Here, $\hat{\mathbf{I}}_{Mn}$ and $\hat{\mathbf{s}}$ are the Mn and electron spins, respectively ($s = 1/2$, $I_{Mn} = 5/2$); $\hat{\mathbf{j}}$ is the HH momentum ($j_h = 3/2$ and $j_{h,z} = \pm 3/2$). The anisotropic e-HH interaction is given by the operator¹⁴:

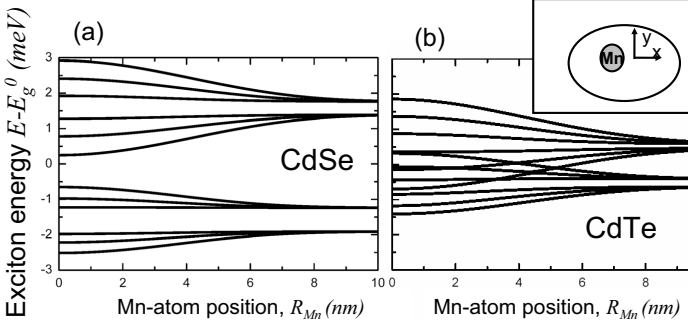


FIG. 1: Exciton energy spectrum as a function of the x -coordinate of the Mn-atom; $R_{Mn,y} = 0$ and $R_{Mn,z} = L_z/2$. The energy E_g^0 is the band gap of a QD. (a) corresponds to $b_x = -0.7$, $b_y = -0.2$, $b_z = -0.4$, and $a_z = -1.2$ meV; (b) corresponds to -0.23 , -0.066 , -0.4 , and -0.13 meV. Insert: geometry of the system.

$$\hat{H}_{e-hole}^{exc} = \sum_{i=x,y,z} a_i \hat{j}_i \hat{s}_i + b_i \hat{j}_i^3 \hat{s}_i, \quad (2)$$

where a_i and b_i are constants. The eigenstates of the Hamiltonian (1) are linear combinations of 24 functions, $|I_{Mn,z}, j_{h,z}, s_{e,z} \rangle$, where $I_{Mn,z}$, $j_{h,z}$, and $s_{z,e}$ are the z-components of the corresponding momenta.

The strength of the Mn-hole and Mn-electron exchange interaction depends on the position of the Mn impurity with respect to the QD (fig. 1, insert) and is given by the coefficients A_h and A_e . For the parameters of exchange interaction, we choose $\alpha N_0 = 0.29$ eV and $\beta N_0 = -1.4$ eV, typical numbers for $II - VI$ materials^{9,12}; here N_0 is the number of cations for unit volume. In fig. 1, we show the calculated spectrum of exciton as a function of the Mn position for two set of parameters a_i and b_i . The first set (fig. 1a) relates to the case of CdSe QD¹⁵ and the second (fig. 1b) corresponds to the weaker e-hole exchange interaction and to a CdTe QD. For the QD wave function, we use a convenient approximation: $\phi_{e(h)}(\mathbf{r}) = B_{e(h)} \sin(\frac{\pi z}{L}) e^{-x^2/l_{x,e(h)}^2 - y^2/l_{y,e(h)}^2}$ ^{16,17}. The sizes of QD are $l_{x,e} = l_{x,h} = 6$ nm, $l_{y,e} = l_{y,h} = 4$ nm, and $L_z = 2$ nm. In fig. 1, we observe that, in the limit $R_{Mn} \rightarrow \infty$, a QD has a spectrum determined by the laterally-anisotropic e-hole exchange interaction; the photoluminescence (PL) spectrum in this case is linearly polarized along the X and Y directions¹⁵. For the case $R_{Mn} \sim l_{dot}$, the energy structure strongly changes due to the Mn-induced exchange interaction that has cylindrical, D_{2d} point-group symmetry. This cylindrical symmetry results in the nonzero spin polarization of the wave functions.

The excitonic wave functions $|\gamma\rangle$ of energies E_γ ($\gamma = 1, 2, \dots, 24$) are doubly degenerate (fig. 1) and their energy spectrum consists of 12 energy levels, $n = 1, 2, \dots, 12$ (fig. 2b). Wave functions in a pair of degenerate states can be written using the two non-crossing subspaces. For example, the states $|1\rangle$ ($|2\rangle$) are composed of

wave functions with $I_{Mn,z} + j_{h,z} + s_{e,z} = 2m + 1/2$ ($I_{Mn,z} + j_{h,z} + s_{e,z} = 2m + 1 + 1/2$), where m is integer.

Master equation. The pumping and PL processes are described by the master equation,

$$\frac{\partial \hat{\rho}}{\partial t} = \frac{i}{\hbar} [\hat{\rho}, \hat{H}_0 + \hat{V}_{opt,+}(t)] + L(\hat{\rho}), \quad (3)$$

where $\hat{\rho}$ is the density matrix, $\hat{V}_{opt,+}(t) = W_0(\hat{p}_+ e^{i\omega_l t} + \hat{p}_- e^{-i\omega_l t})$ is the interaction with classical circularly-polarized light, $\hat{p}_\pm = \hat{p}_x \pm i\hat{p}_y$, and ω_l is the laser frequency. $L(\hat{\rho})$ is the relaxation operator within the Markovian approximation:

$$[L(\hat{\rho})]_{\gamma, \gamma'} = -\frac{\Gamma_\gamma + \Gamma_{\gamma'}}{2} \hat{\rho}_{\gamma, \gamma'} \quad (\gamma \neq \gamma')$$

$$[L(\hat{\rho})]_{\gamma, \gamma} = -\Gamma_\gamma \hat{\rho}_{\gamma, \gamma} + \sum_{\gamma''} \hat{\rho}_{\gamma'', \gamma''} \Gamma_{\gamma'' \rightarrow \gamma}, \quad (4)$$

where $\Gamma_\gamma = \Gamma_\gamma^{intra} + \Gamma_\gamma^{rad}$, Γ_γ^{intra} is the rate of intra-band relaxation of an exciton γ (this relaxation involves both spin and energy), Γ_γ^{rad} is the inter-band, radiative rate. The latter can be written as $\Gamma_\gamma^{rad} = B_\gamma \Gamma_0$, where $\Gamma_0 = 1/\tau_0^{rad}$ is the rate of radiative relaxation for the bright heavy-hole exciton in a QD without a Mn impurity; the coefficient B_γ depends on the spin configuration of the exciton.

The intra-band relaxation rates $\Gamma_{\gamma \rightarrow \gamma'}$ between different momentum and spin states of an exciton depend on a particular system and come from the spin-orbit, electron-phonon, and strong exchange interactions in the conduction and valence bands. In undoped II-VI QDs, the spin relaxation time of an exciton is typically longer than the radiative time. For example, it was found in ref.¹⁸ that the spin relaxation time is longer than 0.5 ns. Ref.¹⁹ reports the hole relaxation time is of order of 10 ps. For our calculations, we take $\Gamma_1 = 1/5$ ns = 0.2 ns⁻¹. For the radiative life-time, we take a typical value $\tau_0^{rad} = 0.5$ ns. At finite temperature T , the rates $\Gamma_{\gamma \rightarrow \gamma'}$ depend on the energy separation $E_{\gamma' \gamma} = E_{\gamma'} - E_\gamma$. Here we will use a simplified model, $\Gamma_{\gamma \rightarrow \gamma'} = \Gamma_1$ if $E_{\gamma' \gamma} < 0$ and $\Gamma_{\gamma \rightarrow \gamma'} = \Gamma_1 e^{-E_{\gamma' \gamma}/k_B T}$ if $E_{\gamma' \gamma} > 0$. This model describes also the thermally-activated transitions. The long spin relaxation time of paramagnetic ions comes from the spin-lattice interaction ($\tau_{spin-lattice} \sim 1 - 100$ ms)²⁰. For the Mn relaxation rate in the absence of an exciton, we choose $\Gamma_{Mn} = 1/10$ ms.

If the light intensity in the pulse is relatively low, the equations (4) are reduced to a system of rate equations for the diagonal components $\rho_\alpha = \rho_{\alpha, \alpha}$, where α can be an exciton-Mn state $|\gamma\rangle$ or a state without exciton, $|I_{Mn,z}\rangle$. In the following, we will be solving numerically a system of rate equations for the two cases. As for the equilibrium density matrix, $\rho_{I_{Mn,z}, I_{Mn,z}}^0 = 1/6$ and otherwise zero.

Circularly-polarized optical emission. The emission intensity of a photo-generated exciton γ is proportional to:

$I_{\pm,\gamma} = (2\pi/\hbar) \sum_{I_{Mn,z}} | < I_{Mn,z} | \hat{V}_{\pm}^{PL} | \gamma > |^2$, where $|\gamma>$ is the initial exciton state, $|I_{Mn,z}>$ are the final states of the system, and $\hat{V}_{\pm}^{PL} = V_0(\hat{p}_x \mp i\hat{p}_x)$ are the operators for the photon emission in the direction $+z$. Then, the degree of circular polarization of a given exciton state γ can be calculated as $P_{circ,\gamma} = (I_{+,\gamma} - I_{-,\gamma})/(I_{+,\gamma} + I_{-,\gamma})$. In the limit $R_{Mn} \rightarrow \infty$ ($A_{e(h)} \rightarrow 0$), the exciton wave functions are determined by the anisotropic e-hole exchange interaction, the emission spectrum is linearly polarized¹⁵, and $P_{circ,\gamma} = 0$. For small R_{Mn} , the calculated degrees $P_{circ,\gamma}$ for excitons in a CdTe QD are close to ± 1 because $A_h > a_i, b_i$. Therefore, the Mn-related symmetric exchange interaction for small R_{Mn} determines the optimal response of excitons.

Since individual excitons have a nonzero degree of circular polarization, PL can also be circularly polarized under the circularly-polarized pumping. We now consider the resonant σ_+ -optical pumping of CdTe QD into a given pair of states with the energy E_γ ($\hbar\omega_l = E_\gamma$) (fig. 2b). Also, we assume a short laser pulse with a duration $\Delta t \ll \tau_{rad}$. The integrated PL intensity of a QD is given by the diagonal components of the density matrix: $I_{PL,\pm} = \int dt (\sum_{\gamma} \rho_{\gamma,\gamma} \Gamma_{\gamma}^{PL,\pm})$, where $\Gamma_{\gamma}^{PL,\pm}$ are the probabilities to emit \pm photons in the vertical direction.

In the limit $R_{Mn} \rightarrow \infty$, the upper bright states can be pumped optically (fig. 2a). Since the individual excitons are linearly polarized, the degree of circular polarization [$P_{circ}^{PL}(\hbar\omega_l = E_\gamma) = (I_{PL,+} - I_{PL,-})/(I_{PL,+} + I_{PL,-})$] is zero.

In the case of $R_{Mn} < \infty$, the time-integrated PL intensity becomes nonzero. In fig. 2, we show the time-integrated PL intensity $I_{PL} = I_{PL,+} + I_{PL,-}$ and P_{circ}^{PL} for all resonant excitations $n = 1, 2, \dots, 12$. The resonance number n in fig. 2c is the number of the exciton energy level counting as shown in fig. 2b. For example, the resonance $n = 1$ relates to the states $\gamma = 1, 2, \dots$. Overall, the circular polarization of PL under circular pumping is well expressed. The circular polarized PL signal was recently recorded in semi-magnetic CdTe QDs¹¹. This observation is in contrast to the previous studies of undoped II-VI and II-V QDs¹⁵. Our theory suggests a qualitative explanation for this observation.

Optical writing and manipulation of the Mn spin. We now calculate the time evolution of Mn spin in the presence of and after a long σ_+ pulse of small intensity ($\Delta t = 0.5 \mu s$, $P_{cv}^2 W_0^2 / \hbar^2 \Gamma_{rad}^2 = 0.02$). In the initial state at $t = 0$, the Mn atom is in thermal equilibrium, $\rho_{I_{Mn,z}} = 1/6$. The evolution of Mn spin strongly depends on how the QD is pumped. As an example, consider the resonance $n = 2$ ($\hbar\omega_l = E_3 = E_4$) and pumping into the exciton states $|3>$ and $|4>$ (fig. 3a,b). The states $|3>$ and $|4>$ optically couple mostly with the Mn states $I_{Mn,z} = \pm 5/2$. Therefore, the σ_+ pulse affects mostly the Mn spin state $I_{Mn,z} = 5/2$. We see that, with increasing time, the probability $\rho_{I_{+5/2}}$ decreases, while $\rho_{I_{-5/2}}$ increases. In this process, the σ_+ pulse excites the state $|4>$, then the exciton $|4>$ makes transition to the state $|3>$, and finally the exciton $|3>$ recombines, contribut-

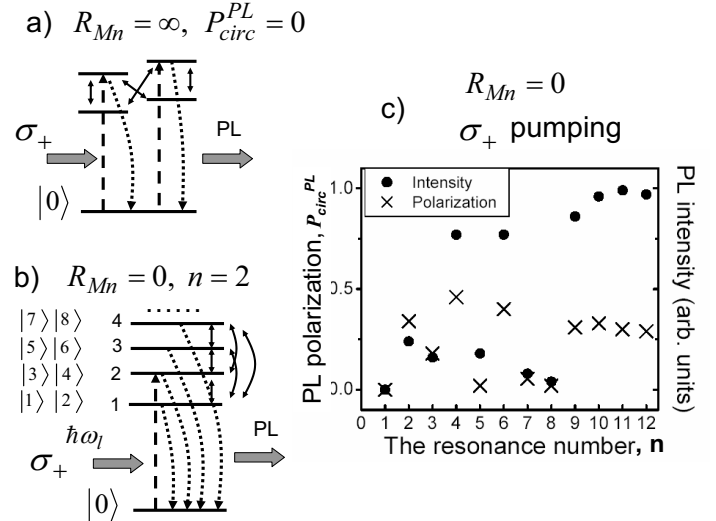


FIG. 2: (a) Exciton spectrum of a QD without a Mn impurity. Arrows show the pumping, emission, and relaxation processes. (b) The pumping and relaxation processes in the presence of a Mn atom; the second level is optically excited, $n = 2$ and $\hbar\omega_l = E_3 = E_4$. (c) Calculated degree of circular polarization and PL intensity for σ_+ pumping in a QD with $R_{Mn} = 0$.

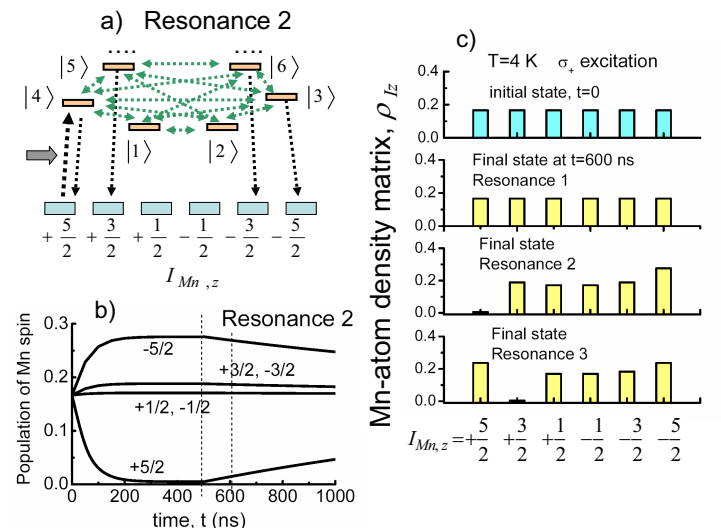


FIG. 3: (a) Schematics of pumping, relaxation, and PL processes in a QD with Mn atom; the second level is resonantly excited $\hbar\omega_l = E_4 = E_3$; here we show only 6 lowest states. (b) Calculated population of Mn atom states as a function of time for the pulse $\Delta t = 0.5 \mu s$. Dashed lines indicate the end of pulse and the measurement time. (c) Population of Mn spin states at $t = 0.6 \mu s$ for different resonant pumping. The initial spin state of Mn is randomized.

ing to the Mn state $I_{Mn,z} = -5/2$. Fig. 3 shows the Mn state at the "measurement" time $t = 0.6 \mu s$. In this way, the Mn spin population becomes non-equilibrium. The exciton ground states $|1>$ and $|2>$ are mostly dark and do not play an important role; they trap and release excitons to the upper energy levels at final T .

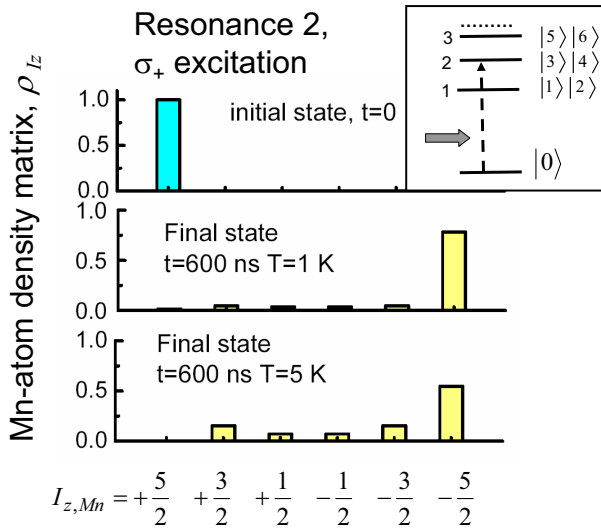


FIG. 4: Population of Mn spin states at $t = 0.6 \mu s$ for the resonant pumping into the second level (insert) at different temperatures. The initial spin state of Mn is $+5/2$.

The optical probing (*reading*) of the state of Mn atom in a QD can be made with the absorption or PLE single-dot spectroscopies which are presently available²². The absorption spectrum of a QD is very sensitive to the Mn spin state^{12,13}. For the σ_{\pm} photons with energy $E_3 = E_4$ ($n = 2$), the light absorption intensity is mostly proportional to $\rho_{I_{\pm 5/2}}$ and thus the change in $\rho_{I_{\pm 5/2}}$ can be recorded.

The non-equilibrium spin distribution $\rho_{I_{Mn}}$ strongly depends on the resonance pumping. The resonant pumping into the ground states $|1\rangle$ and $|2\rangle$ is not efficient since these states are mostly dark (fig. 3c). The resonant pumping $n = 3$ (fig. 3c) results in a decrease of $\rho_{I_{Mn,+3/2}}$ and an increase of $\rho_{I_{Mn,-3/2}}$. Although, the states $\pm 5/2$

become also involved. By using proper resonances, most of the spin Mn states can be addressed in this way. The resonant pumping of a given exciton state can be combined with *Hanbury-Brown/Twiss (HBT) setup*²¹. Consider weak non-resonant illumination of the QD and assume that the QD emits a σ_+ photon with the energy E_4 at $t = 0$. It means that the QD state after the emission process is the Mn state $I_{Mn,z} = +5/2$. This state can then be used as an initial state in our scheme with the polarized laser pulse started at $t = 0$. In the presence of the laser pulse, the Mn state $I_{Mn,z} = +5/2$ turns into the state $I_{Mn,z} = -5/2$ (fig. 4). At the measurement time $t = 0.6 \mu s$, the Mn spin is mostly in the state $I_{Mn,z} = -5/2$. The temperature effect leads to the mixing with other exciton states and more Mn spin states become involved (fig. 4). For the qubit operation in this particular QD, it is logical to choose the Mn spin states $\pm 5/2$ and the resonance E_4 ($n = 2$) since, for this case, the mixing with the other Mn states is minimum. The preparation of qubit in the state $I_{Mn,z} = +5/2$ can be done by detecting a σ_+ photon with the energy E_4 . Then, the rotation of the qubit ($+5/2 \rightarrow -5/2$) can be realized with a polarized laser pulse. The limiting factors are finite temperature and anisotropic electron-hole exchange interaction which create mixing between the qubit and the other states of the Mn spin. The next logical step is to involve two Mn atoms and consider a two-qubit regime.

To conclude, we have studied the optical properties of the spin state of a single magnetic impurity embedded into a semiconductor QD. It is shown that the Mn impurity can be optically manipulated and the impurity spin can act as a qubit.

The author would like to thank Pierre Petroff for motivating discussions. This work was supported by Ohio University and AvH Foundation.

¹ G. A. Prinz, *Science* **282**, 1660 (1998); S. A. Wolf, D. D. Awschalom, R. A. Buhrman, J. M. Daughton, S. von Molnar, M. L. Roukes, A. Y. Chtchelkanova, D. M. Treger, *Science* **294**, 1488 (2001).

² D. Loss and D.P. DiVincenzo, *Phys. Rev. A* **57**, 120 (1998).

³ J. K. Furdina, *J. Appl. Phys.* **65**, 29 (1988).

⁴ *Optical Orientation*, edited by F. Meier and B. P. Zakharchenya (North-Holland, Amsterdam, 1984).

⁵ J. M. Kikkawa and D. D. Awschalom, *Science* **287**, 473 (2000).

⁶ I. A. Merkulov, D. R. Yakovlev, A. Keller, W. Ossau, J. Geurts, A. Waag, G. Landwehr, G. Karczewski, T. Wojtowicz, and J. Kossut, *Phys. Rev. Lett.*, **83**, 1431 (1999).

⁷ H. Krenn, K. Kaltenegger, T. Dietl, J. Spalek, and G. Bauer, *Phys. Rev. B* **39**, 10918 (1989); D. D. Awschalom, J. Warnock and S. von Molnar, *Phys. Rev. Lett.* **58**, 812 (1987); T. Dietl, P. Peyla, W. Grieshaber, and Y. Merle d'Aubigne, *Phys. Rev. Lett.* **74**, 474 (1995).

⁸ J. M. Kikkawa, J. J. Baumberg, D. D. Awschalom, D. Leonard, and P. M. Petroff, *Phys. Rev. B* **50**, 2003 (1994).

⁹ P. S. Dorozhkin, A. V. Chernenko, V. D. Kulakovskii, A. S. Brichkin, A. A. Maksimov, H. Schoemig, G. Bacher, A. Forchel, S. Lee, M. Dobrowolska, and J. K. Furdyna, *Phys. Rev. B* **68**, 195313 (2003).

¹⁰ J. Seufert, G. Bacher, M. Scheibner, A. Forchel, S. Lee, M. Dobrowolska, and J. K. Furdyna, *Phys. Rev. Lett.* **88**, 027402 (2002).

¹¹ S. Mackowski, T. Gurung, T. A. Nguyen, H. E. Jackson, L. M. Smith, G. Karczewski, and J. Kossut, *Appl. Phys. Lett.* **84**, 3337 (2004).

¹² D.M. Hoffman, B.K. Meyer, A.I. Ekimov, I.A. Merkulov, Al. L. Efros, M. Rosen, G. Couino, T. Gacoin, and J.P. Boilot, *Solid State Commun.* **114**, 547 (2000); A. K. Bhattacharjee and J. Perez-Conde, *Phys. Rev. B* **68**, 045303 (2003).

¹³ A. O. Govorov, *Phys. Rev. B*, in press.

¹⁴ E. L. Ivchenko and G. E. Pikus, *Superlattices and Other Heterostructures. Symmetry and Optical Phenomena*

ena (Springer, Berlin, 1997).

¹⁵ V. D. Kulakovskii, G. Bacher, R. Weigand, T. Kummell, A. Forchel, E. Borovitskaya, K. Leonardi, and D. Hommel, Phys. Rev. Lett. **82**, 1780 (1999); M. Bayer, A. Kuther, A. Forchel, A. Gorbunov, V. B. Timofeev, F. Schafer, J. P. Reithmaier, T. L. Reinecke, and S. N. Walck, Phys. Rev. Lett. **82**, 1748 (1999).

¹⁶ R. J. Luyken, A. Lorke, A. O. Govorov, J. P. Kotthaus, G. Medeiros-Ribeiro, and P. M. Petroff, Appl. Phys. Lett. **74**, 2486 (1999).

¹⁷ C. Schulhauser, D. Haft, R. J. Warburton, K. Karrai, A. O. Govorov, A. V. Kalameitsev, A. Chaplik, W. Schoenfeld, J. M. Garcia, and P. M. Petroff, Phys. Rev. B **66**, 193303 (2002).

¹⁸ S. M. Ulrich, S. Strauf, P. Michler, G. Bacher, and A. Forchel, Appl. Phys. Lett., **83**, 1848 (2003).

¹⁹ T. Flissikowski, I. A. Akimov, A. Hundt, and F. Henneberger, Phys. Rev. B **68**, 161309(R) (2003).

²⁰ D. Scalbert, J. Cernogora, and C. Benoit la Guillaume, Solid State Commun. **66**, 571 (1988).

²¹ R. Hanbury-Brown and R. Q. Twiss, Nature (London) **178**, 1447 (1956).

²² J. R. Guest, T. H. Stievater, X. Li, J. Cheng, D. G. Steel, D. Gammon, D. S. Katzer, D. Park, C. Ell, A. Thranhardt, G. Khitrova, and H. M. Gibbs, Phys. Rev. B **65**, 241310 (2002); B. Alen, F. Bickel, K. Karrai, R. J. Warburton, and P. M. Petroff, Appl. Phys. Lett. **83**, 2235 (2003).